Functional characterization of K_v channel β-subunits from rat brain

Stefan H. Heinemann, Jens Rettig*, Hanns-Rüdiger Graack* and Olaf Pongs*

*Max-Planck-Gesellschaft, Arbeitsgruppe Molekulare und zelluläre Biophysik an der Friedrich-Schiller-Universität Jena, Drackendorfer Strasse 1, D-07747 Jena and *Zentrum für Molekulare Neurobiologie Hamburg, Institut für Neurale Signalverarbeitung, D-20246 Hamburg, Germany*

1. The potassium channel β-subunit from rat brain, $K_v\beta1.1$, is known to induce inactivation of the delayed rectifier channel $K_v1.1$ and $K_v1.4\Delta1$–110.

2. $K_v\beta1.1$ was co-expressed in *Xenopus* oocytes with various other potassium channel α-subunits. $K_v\beta1.1$ induced inactivation in members of the K_v1 subfamily with the exception of $K_v1.6$; no inactivation of $K_v2.1$, $K_v3.4\Delta2$–28 and $K_v4.1$ channels could be observed.

3. The second member of the β-subunit subfamily, $K_v\beta2$, had a shorter N-terminal end, accelerated inactivation of the A-type channel $K_v1.4$, but did not induce inactivation when co-expressed with delayed rectifiers of the K_v1 channel family.

4. To test whether this subunit co-assembles with K_v α-subunits, the N-terminal inactivating domains of $K_v\beta1.1$ and $K_v\beta3$ were spliced to the N-terminus of $K_v\beta2$. The chimaeric β-subunits ($\beta1/\beta2$ and $\beta3/\beta2$) induced fast inactivation of several K_v1 channels, indicating that $K_v\beta2$ associates with these α-subunits. No inactivation was induced in $K_v1.3$, $K_v1.6$, $K_v2.1$ and $K_v3.4\Delta2$–28 channels.

5. $K_v\beta2$ caused a voltage shift in the activation threshold of $K_v1.5$ of about −10 mV, indicating a putative physiological role. $K_v\beta2$ had a smaller effect on $K_v1.1$ channels.

6. $K_v\beta2$ accelerated the activation time course of $K_v1.5$ but had no marked effect on channel deactivation.

Depolarization-activated potassium channels (K_v channels) play a major role in shaping the electrical signals in the nervous system. They constitute a large family of channel proteins with quite diverse structural and functional properties (e.g. Chandy & Gutman, 1995). Important features of K_v channels are their threshold of activation and their time course of inactivation. According to their functional properties, K_v channels are roughly classified as delayed rectifier and A-type channels. Delayed rectifier channels open above action potential threshold and inactivate only very slowly, while A-type channels activate at more hyperpolarized voltages and undergo rapid inactivation. On a molecular level, A-type currents can be attributed to K_v channel α-subunits, which give rise to so-called N-type inactivation (Hoshi, Zagotta & Aldrich, 1990). From mammalian brain, several α-subunits with A-type characteristics have been cloned (e.g. $K_v1.4$: Stühmer *et al.* 1989; $K_v3.4$: Schröter, Ruppersberg, Wunder, Rettig, Stocker & Pongs, 1991; $K_v4.1$: Pak, Baker, Covarrubias, Butler, Ratcliffe & Salkoff, 1991). The majority of cloned K_v channel α-subunits, however, give rise to currents of the delayed rectifier type.

We recently cloned K_v channel β-subunits from rat brain. Upon co-expression in *Xenopus* oocytes, $K_v\beta1.1$ transformed non-inactivating delayed rectifier channels, formed by the α-subunits $K_v1.1$ and $K_v1.4\Delta1$–110, into very rapidly inactivating A-type channels (Rettig *et al.* 1994). The homologous β-subunit, $K_v\beta2$, accelerates inactivation of the A-type channel $K_v1.4$ (McCormack, McCormack, Tanouye, Rudy & Stühmer, 1995) but does not induce channel inactivation by itself. N-terminal splice variants of $K_v\beta1.1$ were isolated from ferret heart ($fK_v\beta1.2$: Morales, Castellino, Crews, Rasmusson & Strauss, 1995) and human heart ($hK_v\beta1.2$: England, Uebele, Shear, Kodali, Bennett & Tamkun, 1995; Majumder, Debiasi, Wang & Wible, 1995; notation according to Heinemann, Rettig, Wunder & Pongs, 1995). A homologue to the mammalian K_v β-subunits was cloned from the *hyperkinetic* locus of *Drosophila*; when co-expressed with *Shaker* B channels, it accelerated inactivation and shifted the potential threshold

for activation (Chouinard, Wilson, Schlimgen & Ganetzky, 1995). $K_v\beta3$, the third member of the β-subunit gene family, was cloned from rat brain and induced inactivation in $K_v1.4\Delta1-110$ channels (Heinemann *et al.* 1995). The major differences between $K_v\beta1$, $K_v\beta3$ and $K_v\beta2$ are the longer N-terminal regions of $K_v\beta1$ and $K_v\beta3$, which serve as inactivating structures similar to the 'ball' structure of *Shaker* B potassium channels. Like rat brain A-type channels, $K_v\beta1$ and $K_v\beta3$ subunits harbour a cysteine residue in their N-terminal structure which makes the $K_v\beta$-induced inactivation sensitive to regulation by the intracellular redox potential (Rettig *et al.* 1994; Heinemann *et al.* 1995).

The major functional unit of K_v channels is formed by tetramers of α-subunits (e.g. MacKinnon, 1991) and several different species of α-subunits can co-assemble and thus form hetero-oligomeric channel complexes (e.g. Isacoff, Jan & Jan, 1990; Ruppersberg, Schröter, Sakmann, Stocker, Sewing & Pongs, 1990). Since biochemical analysis showed a tight association of α and β K_v channel subunits in a 1:1 ratio (Parcej, Scott & Dolly, 1992), those K_v channels which co-assemble with $K_v\beta$-subunits may be constituted of four α- and four β-subunits. Therefore, $K_v\beta1.1$ would contribute four N-terminal 'ball' domains for inactivation of the delayed rectifier $K_v1.1$, for example. Although $K_v\beta1.1$ is expressed quite abundantly in rat brain, not all potassium channels measured *in vivo* show inactivation, indicating that not all α-subunits interact with $K_v\beta1.1$. In this study, therefore, we addressed the question of which cloned α-subunits from the K_v channel family form functional complexes with $K_v\beta1.1$.

Since $K_v\beta2$, which lacks an inactivating N-terminal domain, does not induce inactivation, there has so far been no proof for the functional assembly of $K_v\beta2$ with α-subunits other than $K_v1.4$. Therefore we spliced the N-terminal ends of $K_v\beta1.1$ and $K_v\beta3$ to $K_v\beta2$; these modified $K_v\beta2$ subunits caused inactivation when co-expressed with α-subunits with a similar subunit specificity as $K_v\beta1.1$. The unmodified version of $K_v\beta2$ shifted the activation threshold of $K_v1.5$ by about 10 mV to more hyperpolarized voltages, i.e. it conferred activation characteristics to delayed rectifier K_v α-subunits that are typical for A-type channels. In addition, it accelerated activation of $K_v1.5$, while the time course of channel deactivation was not affected.

METHODS

Construction of $K_v\beta$ chimaeras and mRNA synthesis

For the construction of the chimaeras:

$$K_v\beta1.1_{1-110}/K_v\beta2_{77-367}\,(N(K_v\beta1.1)\bullet C(K_v\beta2))$$
$$\text{and } K_v\beta3_{1-117}/K_v\beta2_{77-367}\,(N(K_v\beta3)\bullet C(K_v\beta2)),$$

*Nde*I restriction sites were introduced as silent mutations into pAKS $K_v\beta1.1$, $K_v\beta2$ (Rettig *et al.* 1994) and $K_v\beta3$ (Heinemann *et al.* 1995) cDNA clones at equivalent positions (nucleotide (nt.) 661 in $K_v\beta1.1$ cDNA; nt. 824 in $K_v\beta2$ cDNA; nt. 742 in $K_v\beta3$ cDNA). *In vitro* mutagenesis followed the protocol of Nelson & Long (1989) using the following mutation primers:

5′CACTCTCATATGCAATTGTCA3′ for $K_v\beta1.1$,
5′ATTGTCATATGCCAAGGTC3′ for $K_v\beta2$,
5′CGTGCTCATATGCTACTGT3′ for $K_v\beta3$.

pAKS $K_v\beta2$ (*Nde*I) DNA was cut with *Sph*I and *Nde*I. The resulting *Sph*I/*Nde*I vector was ligated with a *Sph*I/*Nde*I fragment derived from pAKS $K_v\beta1.1$ (*Nde*I) (nt. 1–661 of $K_v\beta1.1$ cDNA) or from pAKS $K_v\beta3$ (*Nde*I) (nt. 1–724 of $K_v\beta3$ cDNA). The chimaeric $K_v\beta$ cDNA clones were checked by sequencing and restriction analysis. mRNAs coding for the β-subunits were prepared as described (Rettig *et al.* 1994).

Electrophysiology

Stage IV–V oocytes were surgically obtained from *Xenopus laevis* anaesthetized with 0·2% tricaine in ice water. The follicular layer was removed manually after treatment with collagenase. mRNA was injected 6–24 h after collagenase treatment and the oocytes were then incubated at 17–18 °C. All other steps for handling of the oocytes were performed according to Stühmer, Terlau & Heinemann (1992).

The concentrations of the mRNAs coding for the α- as well as for the β-subunits were adjusted to 0·25 $\mu g\ \mu l^{-1}$ so that an identical amount of α-subunit mRNA was always injected. Since β-subunit mRNA of the same mass was co-injected, there was a small excess of β over α mRNA molecules due to the smaller molecular weight. The total injection volume was always 50 nl. In some cases, as specified in the text, mRNA coding for the α-subunits was injected at a lower concentration to yield a higher $\beta:\alpha$ ratio.

Between 12 and 48 h after mRNA injection, currents were measured with a two-electrode voltage clamp (Turbo Tec-10CD, npi electronic, Tamm, Germany). Electrodes were filled with 1 M KCl and had resistances between 0·5 and 0·8 MΩ. In most cases the bath medium was normal frog Ringer solution (NFR) with the composition (mM): 115 NaCl, 2·5 KCl, 1·8 $CaCl_2$, 10 Hepes, pH 7·2 (NaOH). For determinations of the voltage dependence of activation, tail current protocols were utilized. In order to slow down tail current kinetics and to permit sizeable inward currents, we used Rb-Ringer solution as the bath solution in these cases, of composition (mM): 115 RbCl, 1·8 $CaCl_2$, 10 Hepes, pH 7·2 (RbOH). All data recordings were performed at room temperature between 18 and 21 °C.

Experiment control, data acquisition and part of the data analysis were performed with the Pulse+PulseFit software package (HEKA Elektronik, Lambrecht, Germany) running on a Macintosh Quadra 650 computer. Leak and capacitive currents were corrected on-line using a P/n correction method. For further data analysis and generation of figures, the program IgorPro (WaveMetrics Inc., Lake Oswego, OR, USA) was used.

All data are expressed as the means ± S.D.

RESULTS

Functional expression of $K_v\beta1$

Xenopus oocytes were used as an expression system for various K_v channel α-subunits and the $K_v\beta1.1$ subunit from rat brain. In the left panel of Fig. 1, outward K^+ currents at +50 mV recorded with the two-electrode clamp

method are shown for various members of the *Shaker*-related K_v1 gene family from rat. While $K_v1.1$, $K_v1.2$, $K_v1.5$ and $K_v1.6$ showed only weak inactivation within the duration of the test pulse, $K_v1.3$ and $K_v1.4\Delta1-110$, a $K_v1.4$ mutant with a deleted N-terminal structure, inactivated within 1 s to about 80–60% of the peak current value, presumably due to slow C-type inactivation. Upon co-expression of these α-subunits with $K_v\beta1.1$, inactivation was induced to a different degree (right panel). While $K_v1.4\Delta1-110$ and $K_v1.5$ inactivated almost completely within a few milliseconds, $K_v1.1$ and $K_v1.2$ inactivated at a similar rate but a significant steady-state current remained. This steady-state current varied considerably between different batches of oocytes. For $K_v1.3$, only a small initial inactivating component could be detected. In three injections we found no effect of $K_v\beta1.1$ on $K_v1.6$ ($n = 17$).

$K_v\beta1.1$ was also co-expressed with $K_v2.1$ (DRK1; Frech, VanDongen, Schuster, Brown & Joho, 1989) ($n = 5$), $K_v3.4\Delta2-28$ (*Raw*3Δ2–28; Rettig *et al.* 1992) ($n = 5$) and $K_v4.1$ (*RShal*; Baldwin, Tsaur, López, Jan & Jan, 1991) ($n = 7$), i.e. members of the gene families related to *Shab*, *Shaw* and *Shal* from *Drosophila* (Covarrubias, Wei & Salkoff, 1991), but no alterations of the inactivation properties of these channels could be observed. Apparently, $K_v\beta1.1$ interacts specifically with members of the K_v1 channel family.

Functional expression of $K_v\beta2$

Outward currents elicited in co-expression experiments of $K_v1.5$ and the β-subunits $K_v\beta1.1$, $K_v\beta2$ and $K_v\beta3$ are shown in Fig. 2 on two time scales. Only $K_v\beta1.1$ induced statistically significant inactivation of $K_v1.5$ channels. Except for the acceleration of inactivation in $K_v1.4$ channels (McCormack *et al.* 1995), no functional properties of $K_v\beta2$ are known so far. Since $K_v\beta2$ has no N-terminal inactivating structure, it is not expected to contribute to channel inactivation via a ball-and-chain mechanism and therefore there is no straightforward assay for expression and assembly with the α-subunits.

In order to equip $K_v\beta2$ with a putative functional entity, we generated constructs by linking cDNA restriction fragments encoding the N-terminal ends of $K_v\beta1.1$ and $K_v\beta3$ to the open reading frame of $K_v\beta2$ cDNA (see Methods). $K_v\beta2$ and the constructs N($K_v\beta1.1$)•C($K_v\beta2$) and N($K_v\beta3$)•C($K_v\beta2$) were co-expressed with $K_v1.5$. Current recordings are shown in Fig. 2, and these indicate that both constructs cause rapid inactivation of $K_v1.5$. This means

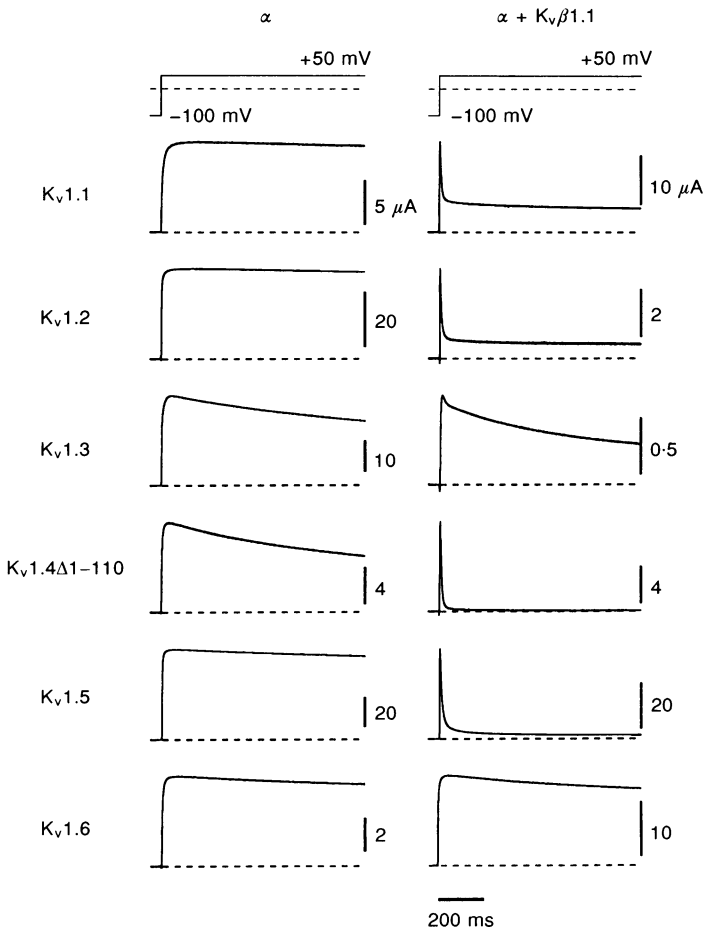

Figure 1. Co-expression of K_v1 α-subunits and $K_v\beta1.1$

Currents were recorded with a two-electrode voltage clamp in response to depolarizing pulses to +50 mV from a holding potential of −100 mV. In the left panel, recordings are shown from oocytes which were injected with mRNA coding for the indicated potassium channel α-subunit. Since $K_v1.4$ codes for an inactivating A-type channel, we used the N-terminal deletion mutant $K_v1.4\Delta1-110$. In the right panel, records obtained from oocytes co-expressing $K_v\beta1.1$ are shown. $K_v\beta1.1$ induces fast inactivation of $K_v1.1$, $K_v1.2$, $K_v1.4\Delta1-110$ and $K_v1.5$ channels. Sequences for the K_v α-subunits used can be found in the following references: $K_v1.1$, $K_v1.2$, $K_v1.3$, $K_v1.4$ and $K_v1.6$, Stühmer *et al.* (1989); $K_v1.5$, Swanson *et al.* (1990).

that $K_v\beta2$ can in fact co-assemble with $K_v1.5$ subunits; provided that it has got an N-terminal inactivating structure, it can also induce inactivation like $K_v\beta1.1$. Interestingly, this is also true for $N(K_v\beta3)•C(K_v\beta2)$, as $K_v\beta3$ does not induce fast inactivation of $K_v1.5$.

The inactivation properties were characterized under two-electrode clamp control with NFR in the bath solution. In Fig. 3*A* the peak currents, normalized to the value at +50 mV, are shown as a function of the test potential, indicating that there are no marked changes in the activation potential. The onset of inactivation was determined at various potentials by fitting exponential functions to the data traces, and only showed a weak voltage dependence (Fig. 3*B*). In some cases, part of the current declined slowly (see Fig. 2), which was accounted for by a second exponential component. The time constants τ_0 and τ_{50} at 0 and +50 mV of the fast components were, for $K_v\beta1.1$: τ_0, 12·7 ± 2·6 ms, τ_{50}, 6·2 ± 0·9 ms ($n = 8$); for $N(K_v\beta1.1)•C(K_v\beta2)$: τ_0, 16·9 ± 3·8 ms, τ_{50}, 5·4 ± 0·7 ms ($n = 12$); and for $N(K_v\beta3)•C(K_v\beta2)$: τ_0, 18·5 ± 2·6 ms, τ_{50}, 8·0 ± 1·2 ms ($n = 8$). Voltage dependence of steady-state inactivation was determined by applying conditioning pulses of 500 ms duration and measuring current at subsequent test pulses to +40 mV (Fig. 3*C*). The voltage dependence was described by a first-order Boltzmann function, characterized by the potential of half-maximal inactivation, V_h, and the slope factor, k. For $K_v\beta1.1$, V_h was −31·5 ± 0·9 mV, k was −3·5 ± 0·1 mV ($n = 7$); for $N(K_v\beta1.1)•C(K_v\beta2)$, V_h was −31·3 ± 0·9 mV, k was −3·5 ± 0·2 mV ($n = 7$); and for $N(K_v\beta3)•C(K_v\beta2)$, V_h was −27·5 ± 1·6 mV, k was −3·4 ± 0·2 mV ($n = 7$). Recovery from inactivation at −100 mV could be described for $K_v\beta1.1$ and $N(K_v\beta1.1)•C(K_v\beta2)$ with a single exponential component with time constants of 2·4 ± 0·4 s ($n = 6$) and 2·7 ± 0·2 s ($n = 3$), respectively. Inactivation induced by $N(K_v\beta3)•C(K_v\beta2)$ recovered with two exponential components having the time constants 0·6 ± 0·1 s and 4·2 ± 0·7 s and a relative weighting of the first component of 0·53 ± 0·08 ($n = 7$) (Fig. 3*D*). $N(K_v\beta3)•C(K_v\beta2)$ also induced inactivation in $K_v1.1$ ($n = 6$), $K_v1.2$ ($n = 7$) and $K_v1.4\Delta1$–110 ($n = 7$) channels but not in $K_v1.3$ ($n = 7$), $K_v1.6$ ($n = 6$), $K_v2.1$ ($n = 3$) and $K_v3.4\Delta2$–28 ($n = 6$) channels. $N(K_v\beta1)•C(K_v\beta2)$ induced inactivation in $K_v1.1$ ($n = 2$) and $K_v1.2$ ($n = 7$) channels but not in $K_v1.3$ ($n = 2$), $K_v1.6$ ($n = 11$) and $K_v2.1$ ($n = 10$) channels. Therefore, with the exception of the recovery from inactivation of $N(K_v\beta3)•C(K_v\beta2)$, the chimaeric β-subunits showed properties which were very similar to those of $K_v\beta1.1$.

$K_v\beta2$ can apparently co-assemble with $K_v1.5$ but normally has no inactivating structure. Therefore the question arises, what role does $K_v\beta2$ play in the functioning of $K_v1.5$?

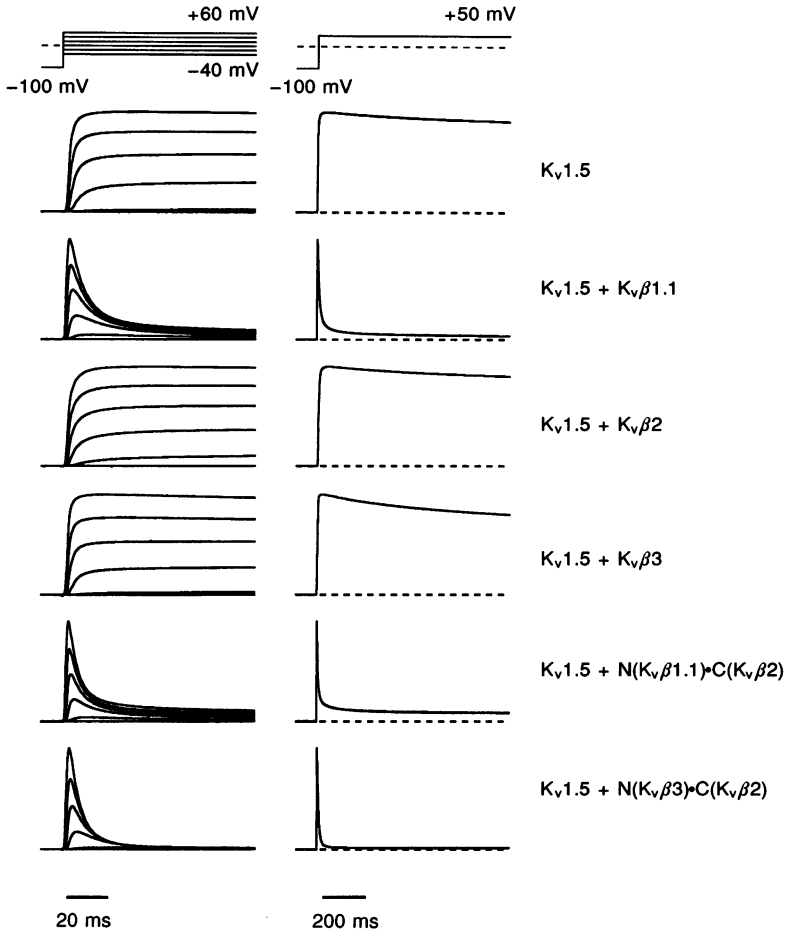

Figure 2. Co-expression of $K_v1.5$ with wild-type $K_v\beta$-subunits and N-terminal chimaeras

Two-electrode clamp recordings were obtained from oocytes expressing $K_v1.5$ α-subunits and the indicated β-subunits. In the left panel, current traces in response to depolarizations ranging from −40 to +60 mV in steps of 20 mV are shown. In the right panel, responses to +50 mV are shown on a compressed time scale. The holding potential was −100 mV. Only $K_v\beta1.1$ of the wild-type β-subunits induces fast inactivation of $K_v1.5$ channels. While $K_v\beta2$ does not influence inactivation of $K_v1.5$, the β-subunit chimaeras, in which the N-terminal ends of $K_v\beta1.1$ or $K_v\beta3$ were linked to the core region of $K_v\beta2$, induce rapid inactivation like $K_v\beta1.1$. Currents were scaled to the peak value, which ranged between 10 and 40 μA.

Since there were no marked kinetic differences between the traces obtained from control $K_v1.5$ oocytes and those which were co-injected with $K_v\beta2$ or $K_v\beta3$ (Fig. 2), we studied the activation properties of these channels in more detail. We injected $\alpha:\beta$ at a ratio of 1 : 2 and measured channel activation and deactivation with NFR as the extracellular solution. As shown in Fig. 4*B*, a small leftward shift in activation potential became apparent after averaging several experiments (here $n = 9$). Steady-state current activation was determined by plotting the peak current as a function of the test potential and fitting a Boltzmann function of the fourth order, accounting for the independent activation of the four channel subunits, characterized by a mid-potential for subunit activation, $V_{½}$, and a slope factor, k . The single-channel conductance was described according to the Goldman–Hodgkin–Katz law (see legend of Fig. 3): for $K_v1.5$, $V_{½}$ was $-18{\cdot}6 \pm 2{\cdot}1$ mV, k was $6{\cdot}5 \pm 0{\cdot}9$ mV ($n = 16$); for $K_v1.5 + K_v\beta2$, $V_{½}$ was $-27{\cdot}1 \pm 1.4$ mV, k was $6{\cdot}6 \pm 0{\cdot}7$ mV ($n = 16$); and for $K_v1.5 + K_v\beta3$, $V_{½}$ was $-18{\cdot}3 \pm 1{\cdot}0$ mV, k was $6{\cdot}2 \pm 0{\cdot}5$ mV ($n = 10$).

The activation time course was estimated by fitting single-exponential functions to the rising phase of the currents (Fig. 4*A*) and the resulting time constants were plotted as squares in Fig. 4*D*. Activation of $K_v1.5$ channels became faster in the presence of $K_v\beta2$, as expected from a shift in

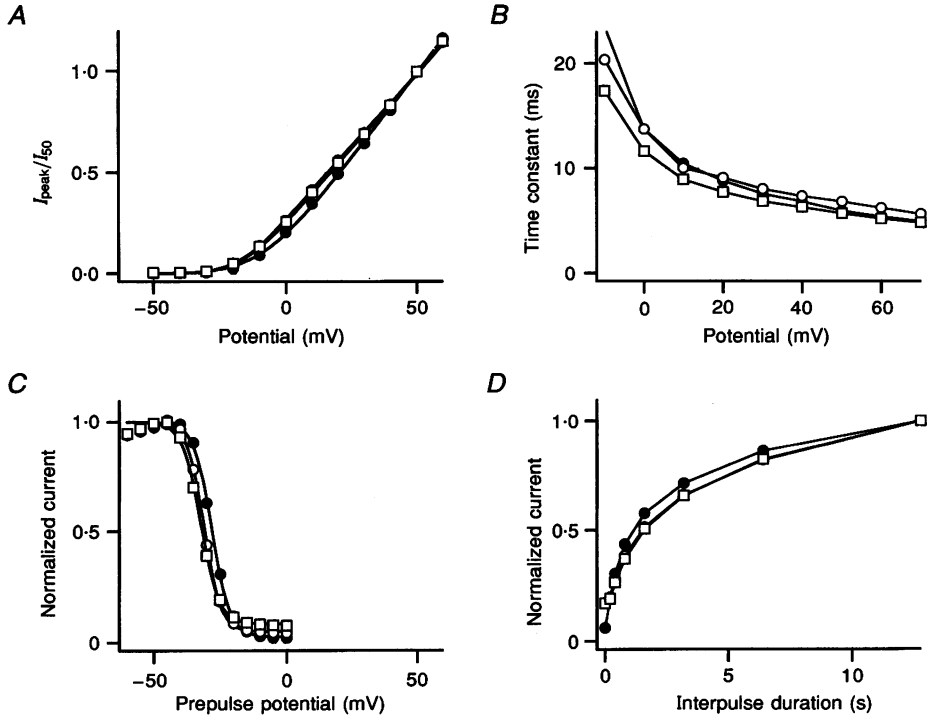

Figure 3. Co-expression of $K_v1.5$ with $K_v\beta1.1$, $N(K_v\beta1.1)•C(K_v\beta2)$ and $N(K_v\beta3)•C(K_v\beta2)$

A, peak currents normalized to the value at +50 mV were recorded from whole oocytes as a function of the test potential for $K_v1.5 + K_v\beta1.1$ (○), $K_v1.5 + N(K_v\beta1.1)•C(K_v\beta2)$ (□) and $K_v1.5 + N(K_v\beta3)•C(K_v\beta2)$ (●). The holding potential was −100 mV and the bath solution contained NFR. The continuous curves indicate data fits according to:

$$I(V) = \Gamma V(1 - \exp(-e_0(V - E_{rev})/k_BT))/(1 - \exp(-e_0V/k_BT))P_{open},$$

with the maximal conductance Γ, the reversal potential $E_{rev} = -90$ mV, the test potential V, and the channel open probability, P_{open}, where

$$P_{open} = (1 + \exp(-(V - V_{½})/k))^{-4}.$$

$V_{½}$ is the half-activation potential per subunit and k is the slope factor; e_0 is the electron charge, k_B is Boltzmann's constant and T the absolute temperature. *B*, time constants of inactivation determined by single-exponential fits as a function of the test potential. The symbols are connected by straight lines. *C*, normalized peak current at +40 mV as a function of the conditioning potential. The continuous curves correspond to first-order Boltzmann fits to the data. The data points are plotted on the same potential scale as those in panel *A* in order to visualize that inactivation coincides with channel opening. *D*, normalized peak current at +40 mV that recovered from inactivation during the indicated interpulse duration at −100 mV. The symbols are connected by straight lines. The use of symbols in *B–D* is the same as in *A*.

activation potential of approximately −10 mV. Activation was additionally described by a current onset according to a fourth power law, accounting for the sigmoidal onset. At +20 mV, the following activation constants were determined: for $K_v1.5$, 3·90 ± 0·35 ms ($n = 17$); for $K_v1.5$ + $K_v\beta2$, 2·59 ± 0·18 ms ($n = 16$); and for $K_v1.5$ + $K_v\beta3$, 3·32 ± 0·14 ms ($n = 9$), indicating that $K_v\beta3$ does not significantly affect activation ($P > 0·1$ for a Student's two-tailed t test). Channel deactivation was measured in tail current experiments by repolarizing from +60 mV to various potentials (Fig. 4*C*). The current decay was described with a single-exponential function, starting after the settling time of the voltage clamp, and the time constants were plotted in Fig. 4*D* as circles. At −40 mV, the following deactivation time constants were determined: for $K_v1.5$, 12·0 ± 1·2 ms ($n = 10$); for $K_v1.5$ + $K_v\beta2$, 12·6 ± 1·7 ms ($n = 12$); and for $K_v1.5$ + $K_v\beta3$, 9·8 ± 1·0 ms ($n = 9$). Thus, deactivation of $K_v1.5$ was not significantly affected by co-expression of these β-subunits ($P > 0·15$).

Since the determination of the steady-state voltage dependence of activation based on outward currents (Fig. 4*A* and *B*) is not very precise, we also applied tail current activation protocols in order to avoid ambiguities with respect to the single-channel properties. Rb-Ringer solution was used as the bathing solution to slow down tail current kinetics. In Fig. 5*A*, current recordings from such a protocol in control conditions and after co-expression of $K_v\beta2$ are shown. In Fig. 5*B*, the normalized peak tail currents are plotted as a function of the potential of the conditioning pulse segment, indicating a shift of channel activation towards more hyperpolarized voltages when $K_v1.5$ is co-expressed with $K_v\beta2$. The continuous curves are Boltzmann fits of the fourth order (see legend of Fig. 5). The voltage shift was close to the limit of resolution, i.e. the variation of the parameters between different batches of oocytes. We therefore determined the activation properties in three independent batches of oocytes in a total of twenty-four experiments for $K_v1.5$ ($V_{½} = -25·7 \pm 2·2$ mV, $k = 7·2 \pm 1·9$ mV) and twenty-three experiments for

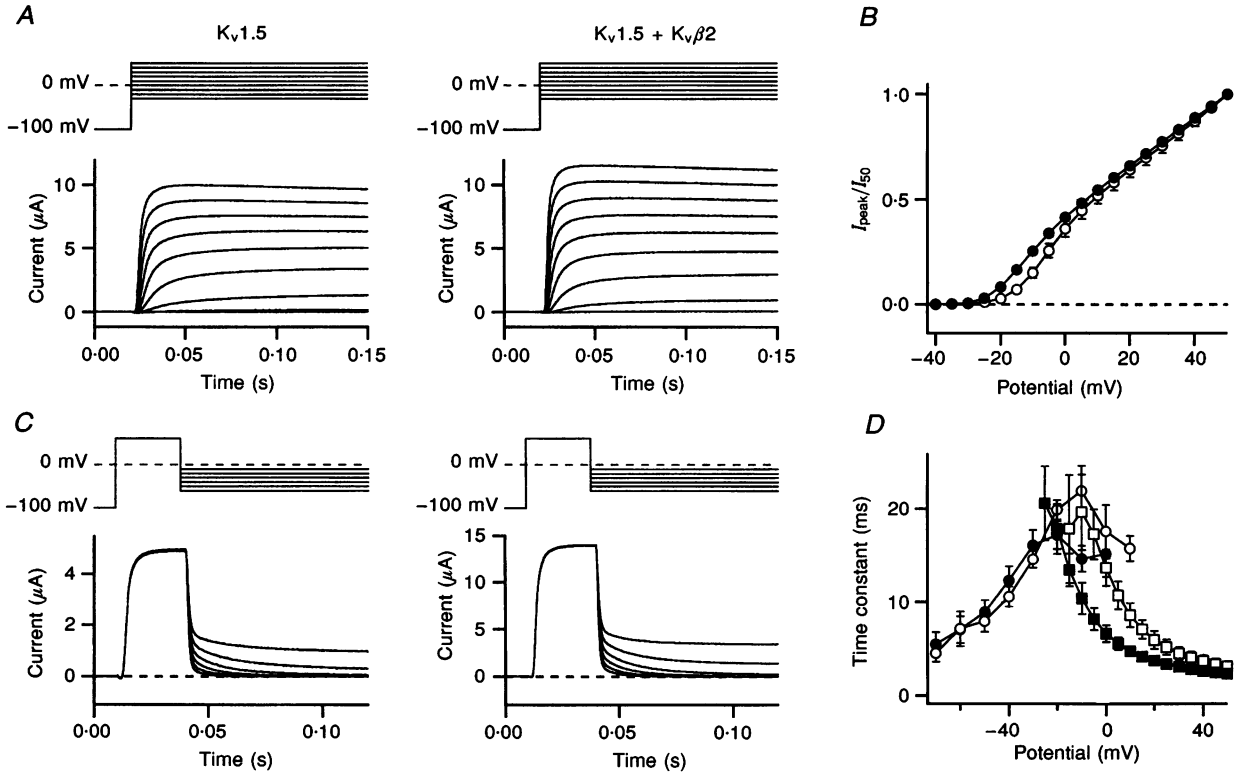

Figure 4. Co-expression of $K_v1.5$ with $K_v\beta2$ affects channel activation

A, current traces recorded from whole oocytes in response to the indicated depolarizing voltage steps ranging from −30 to +50 mV in steps of 10 mV for $K_v1.5$ (left panel) and $K_v1.5$ + $K_v\beta2$ (right panel). The holding potential was −100 mV and the bath solution contained NFR. Maximal currents within a 200 ms pulse were measured and normalized to the value obtained at +50 mV. The means of each nine experiments are plotted in *B* as a function of the test potential ($K_v1.5$, ○; $K_v1.5$ + $K_v\beta2$, ●). The error bars indicate the standard deviation. Kinetics of channel activation were estimated by fitting single-exponential functions to the rising phase of the current traces. The averaged time constants are shown in *D* as squares ($K_v1.5$, □; $K_v1.5$ + $K_v\beta2$, ■). *C*, tail current recordings under the same conditions as described in *A*. The current decay was fitted with single-exponential functions and the mean time constants ($n = 6$ each) are plotted in *D* as circles. The symbols in panels *B* and *D* are connected by straight lines.

$K_v1.5$ co-expressed with $K_v\beta2$ ($V_{½} = -34{\cdot}5 \pm 3{\cdot}0$ mV, $k = 7{\cdot}6 \pm 1{\cdot}7$ mV), yielding a statistically significant shift in $V_{½}$ of $-8{\cdot}8 \pm 3{\cdot}7$ mV ($P < 0{\cdot}018$). The shift of k by $+0{\cdot}4 \pm 2{\cdot}6$ mV was not statistically significant.

Since steady-state activation properties cannot reliably be measured in inactivating channels, a direct comparison of this effect with $K_v\beta1.1$ is not possible. We therefore compared the effects of $K_v\beta2$ and $K_v\beta1.1\Delta1$–34, a $K_v\beta1.1$ subunit with a deleted N-terminal domain (Rettig *et al.* 1994) on the activation of $K_v1.5$ in one batch of oocytes. While the half-activation potential for $K_v1.5$ alone was $-27{\cdot}3 \pm 1{\cdot}8$ mV ($k = 6{\cdot}6 \pm 0{\cdot}4$ mV; $n = 8$), co-expression of $K_v\beta2$ shifted the activation to $-35{\cdot}2 \pm 2{\cdot}6$ mV ($k = 6{\cdot}2 \pm 0{\cdot}5$ mV; $n = 6$) but co-expression of $K_v\beta1.1$-$\Delta1$–34 had an intermediate effect, with a $V_{½}$ of $-31{\cdot}7 \pm 1{\cdot}9$ mV ($k = 7{\cdot}5 \pm 0{\cdot}3$ mV; $n = 4$), which does not reach statistical significance ($P = 0{\cdot}1$).

Co-expression of $K_v\beta2$, $K_v\beta3$ and $K_v\beta1.1\Delta1$–34 with $K_v1.1$ did not result in marked alterations of steady-state activation properties either: for $K_v1.1$, $V_{½}$ was $-41{\cdot}6 \pm 0{\cdot}8$ mV, k was $8{\cdot}4 \pm 1.4$ mV ($n = 5$); for $K_v1.1 + K_v\beta2$, $V_{½}$ was $-45{\cdot}7 \pm 1{\cdot}0$ mV, k was $9{\cdot}5 \pm 0{\cdot}8$ mV ($n = 6$); for $K_v1.1 + K_v\beta1.1\Delta1$–34, $V_{½}$ was $-42{\cdot}3 \pm 0{\cdot}9$ mV, k was $7{\cdot}6 \pm 0{\cdot}8$ mV ($n = 5$); and for $K_v1.1 + K_v\beta3$, $V_{½}$ was $-42{\cdot}4 \pm 1.4$ mV, k was $7{\cdot}8 \pm 1{\cdot}0$ mV ($n = 6$). However, $K_v\beta2$ also accelerated the activation time course of $K_v1.1$, while having no significant effect on deactivation, similar to what was shown in Fig. 4*D* for $K_v1.5$ (data not shown, $n = 6$).

DISCUSSION

Several cDNAs coding for K_v β-subunits have been cloned, forming a gene family (see Heinemann *et al.* 1995). Common to all of these β-subunits is a quite homologous core region with 70–80% sequence identity. The amino-terminal ends are more diverse and vary strongly in length. The amino-termini of $K_v\beta1$ and $K_v\beta3$ subunits contain inactivating domains which function very similarly to the ones found in some K_v α-subunits. One role of K_v β-subunits *in vivo* may, therefore, be to confer A-type characteristics on otherwise non-inactivating potassium channels. This would enable a nerve cell to react flexibly to its incoming stimuli, e.g. by shortening its action potential duration by downregulating the activity of $K_v\beta1$ or $K_v\beta3$.

Due to the lack of an inactivating domain, the role of $K_v\beta2$ is as yet unclear. It was shown to modulate the inactivation time course of $K_v1.4$ (McCormack *et al.* 1995) but it apparently also co-assembles with channels of the delayed rectifier type like $K_v1.5$. Our strategy to prove this was to splice the N-terminal inactivating domain of $K_v\beta1.1$ to $K_v\beta2$. This construct induced fast inactivation in $K_v1.5$ with a time constant similar to the inactivation induced by $K_v\beta1.1$, indicating that $K_v\beta2$ actually assembles with $K_v1.5$. Interestingly, the construct N($K_v\beta3$)•C($K_v\beta2$) induced inactivation in $K_v1.5$ with time constants similar to the inactivation induced by $K_v\beta1.1$ as well, but with a slower recovery from inactivation. This indicates that the lack of inactivation by co-expression of $K_v\beta3$ and $K_v1.5$ is not due to the inability of the $K_v\beta3$ N-terminal 'ball'

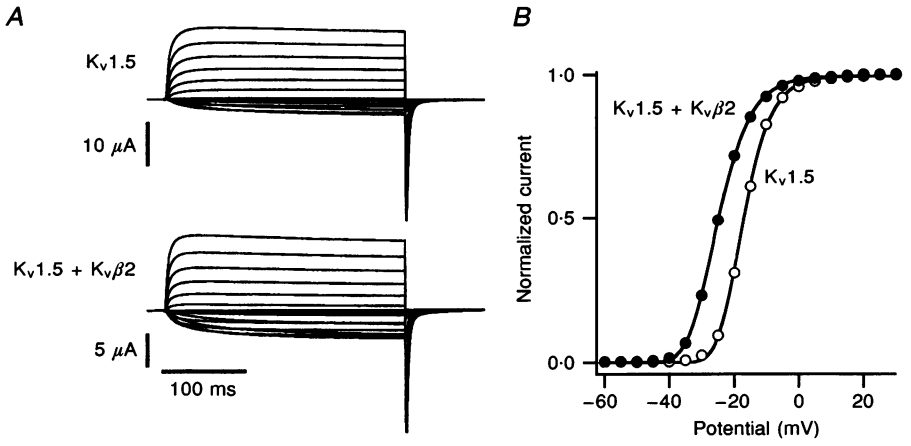

Figure 5. $K_v\beta2$ shifts activation threshold of $K_v1.5$ channels

A, current traces recorded from whole oocytes in response to depolarizing voltage steps ranging from −70 to +40 mV in steps of 5 mV for $K_v1.5$ (top panel) and $K_v1.5 + K_v\beta2$ (bottom panel). The holding and repolarization potential was −100 mV and the bath solution contained Rb-Ringer solution in order to slow down the tail current kinetics. Peak tail currents were measured, normalized to the minimum and plotted in *B* as a function of the test potential. The continuous curves correspond to Boltzmann fits of the fourth order:

$$I/I_{max} = (1 + \exp(-(V - V_{½})/k))^{-4},$$

where V denotes the test potential. In these experiments, the fits yielded for $K_v1.5$: $V_{½} = -25{\cdot}9$ mV, $k = 5{\cdot}4$ mV and for $K_v1.5 + K_v\beta2$: $V_{½} = -35{\cdot}2$ mV, $k = 6{\cdot}3$ mV. For mean values, see text.

structure to bind to $K_v1.5$, but rather an impaired docking of the $K_v\beta3$ subunit to $K_v1.5$. Therefore the C-terminal core sequences may contain the β-subunit interaction site(s) for association with α-subunits.

By functional analysis, we determined that $K_v\beta1.1$ only interacts with channels of the *Shaker*-related K_v1 subfamily. This is consistent with overlay experiments (Sewing, Roeper & Pongs, 1996) which showed that $K_v\beta1.1$ binds to amino-termini of the K_v1 subfamily, but not to those of the K_v2–K_v4 subfamilies. Within the $K_v1.5$ amino-terminus, a $K_v\beta1.1$ interaction site was detected, which is conserved in the K_v1 subfamily. Our results show that $K_v1.6$ channels, in contrast to $K_v1.1$–$K_v1.5$ channels, do not functionally interact with the K_v β-subunits. This finding may indicate that the receptor site of $K_v1.6$ for the inactivation structure is significantly different to those of the other members of the K_v1 channel family. Since the chimaeric channels showed a similar interaction pattern to those of $K_v\beta1.1$ it can be assumed that $K_v\beta2$ binds to the same N-terminal interaction site at the α-subunits as $K_v\beta1.1$.

Co-expression of $K_v\beta2$ with $K_v1.5$ did not result in a change in inactivation properties but caused a small shift of steady-state activation by about −10 mV. A similar shift was reported by England *et al.* (1995) to occur after co-expression of $hK_v\beta1.2$ and $hK_v1.5$ and by Chouinard *et al.* (1995) after co-expression of *hyperkinetic* and *Shaker* BΔ6–46, albeit in the presence of inactivation. We found no significant shift when co-expressing $K_v\beta1.1$ without the N-terminal domain ($K_v\beta1.1\Delta1$–34) or $K_v\beta3$ with $K_v1.5$, indicating that $K_v\beta2$ has the strongest influence on the channel activation mechanism. Further insight is provided by the result that $K_v\beta2$ accelerates the activation time course without affecting channel deactivation. Although these effects need to be studied with higher time resolution in patch-clamp studies, they suggest an interaction of $K_v\beta2$ with early steps in channel activation, such as those involving rearrangements of the S4-segment, which are known to be accessible from the intracellular side of the membrane (Starkus, Schlief, Rayner & Heinemann, 1995).

In terms of activation properties, $K_v\beta2$ confers one characteristic of A-type channels, namely a low potential threshold for activation, to the delayed rectifier $K_v1.5$ channel which has a high threshold for activation. $K_v1.1$ already has a low activation threshold and no significant shift in activation potential was observed when $K_v\beta2$ was co-expressed. Further studies are required to show whether this is one of the significant physiological roles of $K_v\beta2$ in rat brain.

Baldwin, T. J., Tsaur, M. L., López, L. A., Jan, Y. N. & Jan, L. Y. (1991). Characterization of a mammalian cDNA for an inactivating voltage-sensitive K^+ channel. *Neuron* **7**, 471–483.

Chandy, K. G. & Gutman, G. A. (1995). Voltage gated K^+ channel genes. In *Handbook of Receptors and Channels*, ed. North, R. A., pp. 1–71. CRC Press, Boca Raton, FL, USA.

Chouinard, S. W., Wilson, G. F., Schlimgen, A. K. & Ganetzky, B. (1995). A potassium channel β subunit related to the aldo-keto reductase superfamily is encoded by the *Drosophila* Hyperkinetic locus. *Proceedings of the National Academy of Sciences of the USA* **92**, 6763–6767.

Covarrubias, M., Wei, A. & Salkoff, L. (1991). *Shaker, Shal, Shab* and *Shaw* express independent K^+ current systems. *Neuron* **7**, 763–773.

England, S. K., Uebele, V. N., Shear, H., Kodali, J., Bennett, P. B. & Tamkun, M. M. (1995). Characterization of a voltage-gated K^+ channel β-subunit expressed in human heart. *Proceedings of the National Academy of Sciences of the USA* **92**, 6309–6313.

Frech, G. C., VanDongen, A. M., Schuster, G., Brown, A. M. & Joho, R. H. (1989). A novel potassium channel with delayed rectifier properties isolated from rat brain by expression cloning. *Nature* **340**, 642–645.

Heinemann, S. H., Rettig, J., Wunder, F. & Pongs, O. (1995). Molecular and functional characterization of a rat brain $K_v\beta3$ potassium channel subunit. *FEBS Letters* **377**, 383–389.

Hoshi, T., Zagotta, W. N. & Aldrich, R. W. (1990). Biophysical and molecular mechanisms of *Shaker* potassium channel inactivation. *Science* **250**, 533–538.

Isacoff, E. Y., Jan, Y. N. & Jan, L. Y. (1990). Evidence for the formation of heteromultimeric potassium channels in *Xenopus* oocytes. *Nature* **345**, 530–534.

McCormack, K., McCormack, T., Tanouye, M., Rudy, B. & Stühmer, W. (1995). Alternative splicing of the human *Shaker* K^+ channel $\beta1$ gene and functional expression of the $\beta2$ gene product. *FEBS Letters* **370**, 32–36.

MacKinnon, R. (1991). Determination of the subunit stoichiometry of a voltage-activated potassium channel. *Nature* **350**, 232–235.

Majumder, K., Debiasi, M., Wang, Z. & Wible, B. A. (1995). Molecular cloning and functional expression of a novel potassium channel β-subunit from human atrium. *FEBS Letters* **361**, 13–16.

Morales, M. J., Castellino, R. C., Crews, A. L., Rasmusson, R. L. & Strauss, H. C. (1995). A novel β-subunit increases rate of inactivation of specific voltage-gated potassium channel α-subunits. *Journal of Biological Chemistry* **270**, 6272–6277.

Nelson, R. M. & Long, G. L. (1989). A general method of site-specific mutagenesis using a modification of the *Thermus aquaticus* polymerase chain reaction. *Analytical Biochemistry* **180**, 147–151.

Pak, M. D., Baker, K., Covarrubias, M., Butler, A., Ratcliffe, A. & Salkoff, L. (1991). mShal, a subfamily of A-type K^+ channel cloned from mammalian brain. *Proceedings of the National Academy of Sciences of the USA* **88**, 4386–4390.

Parcej, D. N., Scott, V. E. S. & Dolly, J. O. (1992). Oligomeric properties of α-dendrotoxin-sensitive potassium ion channels purified from bovine brain. *Biochemistry* **31**, 11084–11088.

Rettig, J., Heinemann, S. H., Wunder, F., Lorra, C., Parcej, D. N., Dolly, O. & Pongs, O. (1994). Inactivation properties of voltage-gated K^+ channels altered by presence of β-subunit. *Nature* **369**, 289–294.

Rettig, J., Wunder, F., Stocker, M., Lichtinghagen, R., Mastiaux, F., Beckh, S., Kues, W., Pedarzani, P., Schröter, K. H., Ruppersberg, J. P., Veh, R. & Pongs, O. (1992). Characterization of a *Shaw*-related potassium channel family in rat brain. *EMBO Journal* **11**, 2473–2486.

Ruppersberg, J. P., Schröter, K. H., Sakmann, B., Stocker, M., Sewing, S. & Pongs, O. (1990). Heteromultimeric channels formed by rat brain potassium-channel proteins. *Nature* **345**, 535–537.

Schröter, K. H., Ruppersberg, J. P., Wunder, F., Rettig, J., Stocker, M. & Pongs, O. (1991). Cloning and functional expression of a TEA-sensitive A-type potassium channel from rat brain. *FEBS Letters* **278**, 211–216.

Sewing, S., Roeper, J. & Pongs, O. (1996). $K_v\beta1$-subunit binding specific for *Shaker*-related potassium channel α-subunits. *Neuron* **16**, 455–463.

Starkus, J. G., Schlief, T., Rayner, M. D. & Heinemann, S. H. (1995). Unilateral exposure of *Shaker* B potassium channels to hyperosmolar solutions. *Biophysical Journal* **69**, 860–872.

Stühmer, W., Ruppersberg, J. P., Schröter, K. H., Sakmann, B., Stocker, M., Giese, K. P., Perschke, A., Baumann, A. & Pongs, O. (1989). Molecular basis of functional diversity of voltage-gated potassium channels in mammalian brain. *EMBO Journal* **8**, 3235–3244.

Stühmer, W., Terlau, H. & Heinemann, S. H. (1992). Two electrode and patch clamp recording from *Xenopus* oocytes. In: *Practical Electrophysiological Methods*, ed. Kettenmann, H. & Grantyn, R., pp. 121–125. Wiley-Liss, New York.

Swanson, J. S., Marshall, J., Smith, J. S., Williams, J. B., Boyle, M. B., Folander, K., Luneau, C. J., Anatanavage, J., Olivia, C., Behrow, S. A., Bennet, C., Stein, R. B. & Kaczmarek, L. K. (1990). Cloning and expression of cDNA and genomic clones encoding three delayed-rectifier potassium channels in rat brain. *Neuron* **4**, 929–939.

Acknowledgements

O.P. thanks K. Weber for her invaluable help in mRNA synthesis and the Deutsche Forschungsgemeinschaft for support. S.H.H. thanks A. Roßner for preparation of *Xenopus* oocytes.

Authors' present addresses

J. Rettig: Max-Planck-Institut für biophysikalische Chemie, Abt. 140, Am Faßberg, D-37077 Göttingen, Germany.

H.-R. Graack: Institut für Genetik, Freie Universität Berlin, Arnimallee 7, D-14195 Berlin, Germany.

Author's email address

S. H. Heinemann: ite@rz.uni-jena.de

Received 10 October 1995; accepted 9 February 1996.